



Linear and energy stable schemes for the Swift–Hohenberg equation with quadratic-cubic nonlinearity based on a modified scalar auxiliary variable approach

Junxiang Yang · Junseok Kim

Received: 24 June 2020 / Accepted: 4 March 2021 / Published online: 2 June 2021
© The Author(s), under exclusive licence to Springer Nature B.V. 2021

Abstract In this study, we develop linear and energy stable numerical schemes for the Swift–Hohenberg equation with quadratic-cubic nonlinearity. A modified scalar auxiliary variable (SAV) approach is used to construct the temporally first- and second-order accurate discretizations. Different from the classical SAV approach, the proposed schemes permit us to solve the governing equations in a step-by-step manner, i.e., the calculation of inner product is not needed. We analytically prove the energy stability. We solve the resulting system of discrete equations using the linear multigrid method. We perform various numerical examples to show the accuracy and energy stability of the proposed method. The pattern formations in two- and three-dimensional spaces are also simulated.

Keywords Energy stability · Pattern formation · SAV approach · Swift–Hohenberg equation

1 Introduction

In this article, we consider the Swift–Hohenberg (SH) equation with quadratic-cubic nonlinearity [1–3]:

$$\phi_t = -(\phi^3 - g\phi^2 + (-\epsilon + (1 + \Delta)^2)\phi), \quad (1)$$

where $\phi = \phi(\mathbf{x}, t)$ is the density field in the domain $\mathbf{x} \in \Omega \subset \mathbb{R}^d$, where $d = 2$ or 3 is the space dimension and the subscript t represents the derivative with respect to time t , g is a nonnegative constant, ϵ is a positive parameter, and $\epsilon < 1$ in general. The SH equation has extensive applications in physical and industrial fields, such as biological tissue [4], thermal convection [1], crystallography [5], and pattern formations [6]. One can derive the SH equation (1) by taking the variational derivative of the following energy functional:

$$\mathcal{E}(\phi) = \int_{\Omega} \left(\frac{1}{4}\phi^4 - \frac{g}{3}\phi^3 + \frac{1}{2}\phi(-\epsilon + (1 + \Delta)^2)\phi \right) dx. \quad (2)$$

We take the derivative of Eq. (2) with respect to time t and we obtain

$$\frac{d}{dt} \mathcal{E}(\phi) = - \int_{\Omega} \phi_t^2 dx \leq 0,$$

which indicates the energy functional of the SH equation is nonincreasing. To numerically study the dynamics of the SH equation, one important criterion of constructing numerical scheme is whether the energy dissipation law

J. Yang · J. Kim (✉)
Department of Mathematics, Korea University, Seoul 02841, Republic of Korea
e-mail: cfdkim@korea.ac.kr

is satisfied at larger time steps. In the past thirty years, many scholars have developed various practical numerical schemes for the SH equation [7–12]. However, most of the previous works only have first-order temporal accuracy. To obtain the desired results under larger time steps, high-order (at least second-order) accurate schemes are necessary. Sarmiento et al. [13] developed an adaptive second-order accurate and energy stable method for the SH model with controllable dissipation. Lee [14] proposed a high-order semi-analytical Fourier spectral method for the SH equation. Su et al. [5] numerically studied the SH equation by using a compact difference method. Their works only focus on the case of $g = 0$ (no cubic nonlinearity). Note that the case of $g \neq 0$ usually causes some challenges in constructing energy stable numerical schemes. Based on the idea of convex splitting, Lee [3] recently proposed nonlinearly energy stable schemes for the SH equation. Here, the nonlinear part is treated implicitly and Newton-type linearization is needed in the iteration. Moreover, the convex splitting method has been successfully applied to various phase-field models with SH-type free energy. For example, Wise et al. [15] developed an unconditionally stable finite-difference scheme for the phase-field crystal (PFC) equation. Hu et al. [16] proposed an efficient and energy stable nonlinear-multigrid method for solving the PFC model. Guan et al. [17] developed a hexagonal finite difference scheme for the PFC amplitude equations in two-dimensional space. Wang and Wise [18] developed an energy stable finite difference method for the modified PFC equation by using the convex splitting approach. Later, Baskaran et al. [19] proposed an efficient and stable nonlinear-multigrid method for solving the modified PFC model. Cheng et al. [20] constructed an energy stable scheme for the square PFC equation by using the Fourier pseudo-spectral method and BDF2 temporal discretization. For more details of convergence and error estimations of second-order convex splitting methods for three-dimensional PFC model and modified PFC model, please refer to [21,22].

In this work, we want to develop the desired numerical schemes satisfying the following advantages: (1) Accuracy (at least second-order accuracy), (2) Energy stability (the energy dissipation law is satisfied), and (3) Efficiency (linear system with constant coefficients), for the Allen–Cahn (AC) equation [23–26], Cahn–Hilliard (CH) equation [27,28], PFC equation [29], etc. The recently developed Lagrange multiplier approach [30], invariant energy quadratization (IEQ) approach [31], and scalar auxiliary variable (SAV) approach [32] are the popular ways to construct efficient and energy stable schemes with high-order accuracy. The classical Lagrange multiplier approach is valid for the problems with fourth-order polynomial potential, such as the AC, CH, and PFC equations [30,33]. One can use an auxiliary variable to replace the quadratic nonlinear terms in the equation to construct energy stable schemes. For the SH equation with cubic nonlinearity, it is hard to show the energy stability if we replace all quadratic parts with an auxiliary variable. For the IEQ and SAV approaches, we admit that they not only satisfy the energy dissipation law for various gradient flows, but also naturally satisfy the boundedness of total energy because the auxiliary variable is defined in the form of square-root. They are good methods for the phase-field models with nonlinear terms satisfying the bounded-from-below condition. However, if we consider the SH equation with cubic nonlinearity, there is no criterion guiding us to choose an exact constant to guarantee the term beneath the square-root be always positive because the variable $g > 0$. If an improper constant is used, the value beneath the square-root may be negative, and then the computation cannot be conducted. Therefore, for the SH equation in the case of $g \neq 0$, the classical Lagrange multiplier, IEQ, and SAV approaches may be not very practical [34]. In a recent work of Liu and Li [35], a step-by-step solving scheme based on the SAV approach was proposed for the AC, CH, and PFC equations. This new approach weakens the condition of classical SAV approach and inherits the advantages of classical SAV approach. The similar ideas can also be found in a recent work [36] for phase-field surfactant model.

Inspired by the ideas in [35], we develop linear and energy stable numerical schemes for the SH equation with $g \geq 0$. In our schemes, the bounded below restriction of classical SAV approach is weakened, i.e., we only require that the auxiliary variable is not zero. Moreover, the density field ϕ and auxiliary variable are decoupled with each other, and thus we can solve them in a step-by-step way, i.e., the density field is updated by solving only one semi-implicit system with constant coefficients and then the auxiliary variable can be directly updated by an explicit way. Different with the classical SAV approach, the calculation of inner product is not needed any more, the whole algorithm is significantly simplified. To the best of our knowledge, this is the first work using the modified SAV approach [35] to treat the SH equation with $g \geq 0$.

The organization of the rest of this work is as follows. In Sect. 2, we describe the equivalent form of governing equations. In Sect. 3, we present the temporally first- and second-order accurate schemes and analytically estimate the energy dissipation law. In Sect. 4, various computational experiments are performed. The conclusion are given in Sect. 5.

2 Governing equations

In this section, we describe the equivalent governing equations based on the improved SAV approach. Defining the following auxiliary variable

$$U = E(\phi) + C, \tag{3}$$

where $E(\phi) = \int_{\Omega} (\frac{1}{4}\phi^4 - \frac{g}{3}\phi^3 - \frac{\epsilon}{2}\phi^2) dx$ and C is a constant ensuring $E(\phi) + C \neq 0$. Based on the property $\mathcal{E}(\phi^0) \geq \mathcal{E}(\phi)$, where $\mathcal{E}(\phi^0)$ is the initial total energy functional, we can find

$$\mathcal{E}(\phi^0) - E(\phi) = \mathcal{E}(\phi^0) - \mathcal{E}(\phi) + \int_{\Omega} \frac{1}{2}\phi(1 + \Delta)^2\phi dx \geq 0. \tag{4}$$

Thus, we can use $C = -\mathcal{E}(\phi^0) - \gamma$, where γ is any positive constant and we use $\gamma = 0.0001$ in this work. Therefore, the total energy function (2) can be written to be the following equivalent form:

$$\begin{aligned} \mathcal{E}(\phi, U) &= \int_{\Omega} \frac{1}{2}\phi(1 + \Delta)^2\phi dx + U - C \\ &= \int_{\Omega} \frac{1}{2}\phi^2 - |\nabla\phi|^2 + \frac{1}{2}(\Delta\phi)^2 dx + U - C, \end{aligned} \tag{5}$$

where the periodic boundary condition is considered. By taking the variational derivative of Eq. (5) with respect to ϕ and taking the derivative of U with respect to time t , we derive the following equivalent governing equations:

$$\phi_t = -\frac{U}{E(\phi) + C} F'(\phi) - \phi - 2\Delta\phi - \Delta\kappa, \tag{6}$$

$$\kappa = \Delta\phi, \tag{7}$$

$$U_t = \int_{\Omega} \frac{U}{E(\phi) + C} F'(\phi)\phi_t dx, \tag{8}$$

where $F(\phi) = \frac{1}{4}\phi^4 - \frac{g}{3}\phi^3 - \frac{\epsilon}{2}\phi^2$ and $F'(\phi)$ represents the derivative with respect to ϕ . By taking the inner product of Eq. (6) with $-\phi_t$, we have

$$-\|\phi_t\|^2 = \left(\frac{U}{E(\phi) + C} F'(\phi), \phi_t \right) + (\phi, \phi_t) + (2\Delta\phi, \phi_t) + (\Delta\kappa, \phi_t), \tag{9}$$

where $(a, a) = \|a\|^2$ is the L^2 -inner product.

By taking the inner product of Eq. (7) with $\Delta\phi_t$, we get

$$(\kappa, \Delta\phi_t) = (\Delta\kappa, \phi_t) = (\Delta\phi, \Delta\phi_t). \tag{10}$$

By combining Eqs. (9) and (10) and using Eq. (8), we obtain

$$\frac{d}{dt} U + \frac{1}{2} \frac{d}{dt} \|\phi\|^2 - \frac{d}{dt} \|\nabla\phi\|^2 + \frac{1}{2} \frac{d}{dt} \|\Delta\phi\|^2 = -\|\phi_t\|^2 \leq 0, \tag{11}$$

which implies the equivalent total energy functional (5) satisfies the energy dissipation law. Here, we adopt the periodic boundary condition or the following homogeneous Neumann boundary condition:

$$\nabla\phi \cdot \mathbf{n}|_{\partial\Omega} = 0, \quad \nabla\kappa \cdot \mathbf{n}|_{\partial\Omega} = 0,$$

where \mathbf{n} is the unit outward vector to the domain boundary $\partial\Omega$. Based on the equivalent governing equations (6)–(8), we will construct linearly first- and second-order schemes in the next section. For the energy stable schemes, the periodic and the above homogeneous Neumann boundary conditions are commonly used because the effects from boundary can be easily removed. Recently, Espath et al. [37] proposed generalized SH models based on a second-gradient phase-field theory with general boundary condition. For a general boundary condition, some technical works are needed to construct energy stable scheme and we will consider this interesting issue in the future.

3 Proposed temporal schemes

3.1 Linearly first-order scheme (LS1)

For Eqs. (6)–(8), we propose the following temporally first-order accurate numerical scheme

$$\frac{\phi^{n+1} - \phi^n}{\Delta t} = -\frac{U^n}{E(\phi^n) + C} F'(\phi^n) - \phi^{n+1} - 2\Delta\phi^n - \Delta\kappa^{n+1}, \tag{12}$$

$$\kappa^{n+1} = \Delta\phi^{n+1}, \tag{13}$$

$$\frac{U^{n+1} - U^n}{\Delta t} = \int_{\Omega} \frac{U^n}{E(\phi^n) + C} F'(\phi^n) \frac{\phi^{n+1} - \phi^n}{\Delta t} d\mathbf{x}, \tag{14}$$

where superscripts $n + 1$ and n represent the solutions at $n + 1$ and n time level, and Δt is the time step. Next, we prove the proposed first-order scheme (12)–(14) satisfies the discrete energy dissipation law, i.e., $\mathcal{E}(\phi^{n+1}, U^{n+1}) \leq \mathcal{E}(\phi^n, U^n)$, where

$$\mathcal{E}(\phi^n, U^n) = U^n + \frac{1}{2} \|\phi^n\|^2 - \|\nabla\phi^n\|^2 + \frac{1}{2} \|\Delta\phi^n\|^2 - C.$$

By taking the inner product of Eq. (12) with $-(\phi^{n+1} - \phi^n)$, we have

$$-\frac{1}{\Delta t} \|\phi^{n+1} - \phi^n\|^2 = \left(\frac{U^n}{E(\phi^n) + C}, \phi^{n+1} - \phi^n \right) + (\phi^{n+1}, \phi^{n+1} - \phi^n) + (2\Delta\phi^n, \phi^{n+1} - \phi^n) + (\Delta\kappa^{n+1}, \phi^{n+1} - \phi^n). \tag{15}$$

By using the following identity:

$$(a, a - b) = \frac{1}{2} (|a|^2 - |b|^2 + |a - b|^2),$$

we can rewrite Eq. (16) to be

$$-\frac{1}{\Delta t} \|\phi^{n+1} - \phi^n\|^2 = \left(\frac{U^n}{E(\phi^n) + C}, \phi^{n+1} - \phi^n \right) + \frac{1}{2} (\|\phi^{n+1}\|^2 - \|\phi^n\|^2 - \|\phi^{n+1} - \phi^n\|^2) + (\|\nabla\phi^n\|^2 - \|\nabla\phi^{n+1}\|^2 + \|\nabla\phi^n - \nabla\phi^{n+1}\|^2) + (\Delta\kappa^{n+1}, \phi^{n+1} - \phi^n). \tag{16}$$

By taking the inner product of Eq. (13) with $\Delta(\phi^{n+1} - \phi^n)$, we obtain

$$(\kappa^{n+1}, \Delta(\phi^{n+1} - \phi^n)) = (\Delta\kappa^{n+1}, \phi^{n+1} - \phi^n) = \frac{1}{2} (\|\Delta\phi^{n+1}\|^2 - \|\nabla\phi^n\|^2 + \|\Delta\phi^{n+1} - \Delta\phi^n\|^2). \tag{17}$$

By combine Eqs. (16) and (17) and using Eq. (14), we obtain

$$U^{n+1} - U^n + \frac{1}{2} \|\phi^{n+1}\|^2 - \frac{1}{2} \|\phi^n\|^2 - \|\nabla\phi^{n+1}\|^2 + \|\nabla\phi^n\|^2 + \frac{1}{2} \|\Delta\phi^{n+1}\|^2 - \frac{1}{2} \|\Delta\phi^n\|^2 = -\frac{1}{\Delta t} \|\phi^{n+1} - \phi^n\|^2 - \frac{1}{2} \|\phi^{n+1} - \phi^n\|^2 - \frac{1}{2} \|\Delta\phi^{n+1} - \Delta\phi^n\|^2 \leq 0, \tag{18}$$

which implies $\mathcal{E}(\phi^{n+1}, U^{n+1}) \leq \mathcal{E}(\phi^n, U^n)$, and the discrete energy dissipation law is proved.

3.2 Linearly second-order scheme (LS2)

For Eqs. (6)–(8), the proposed temporally second-order accurate scheme is written to be

$$\frac{\phi^{n+1} - \phi^n}{\Delta t} = -\frac{U^*}{E(\phi^*) + C} F'(\phi^*) - \frac{\phi^{n+1} + \phi^n}{2} - 2\Delta\phi^* - \Delta\kappa^{n+\frac{1}{2}}, \tag{19}$$

Table 1 Convergence rates and L^2 -errors with different time steps

Δt	LS1	Order	LS2	Order
$320\Delta t^r$	$6.56e-2$	—	$5.96e-2$	—
$160\Delta t^r$	$3.32e-2$	0.98	$1.55e-2$	1.94
$80\Delta t^r$	$1.66e-2$	1.00	$4.00e-3$	1.95
$40\Delta t^r$	$8.20e-3$	1.02	$1.00e-3$	2.00
$20\Delta t^r$	$4.00e-3$	1.04	$2.54e-4$	1.98
$10\Delta t^r$	$1.90e-3$	1.07	$6.34e-5$	2.00

The numerical reference solution is obtained with $\Delta t^r = 3.2h^2$ at $t = 0.1$

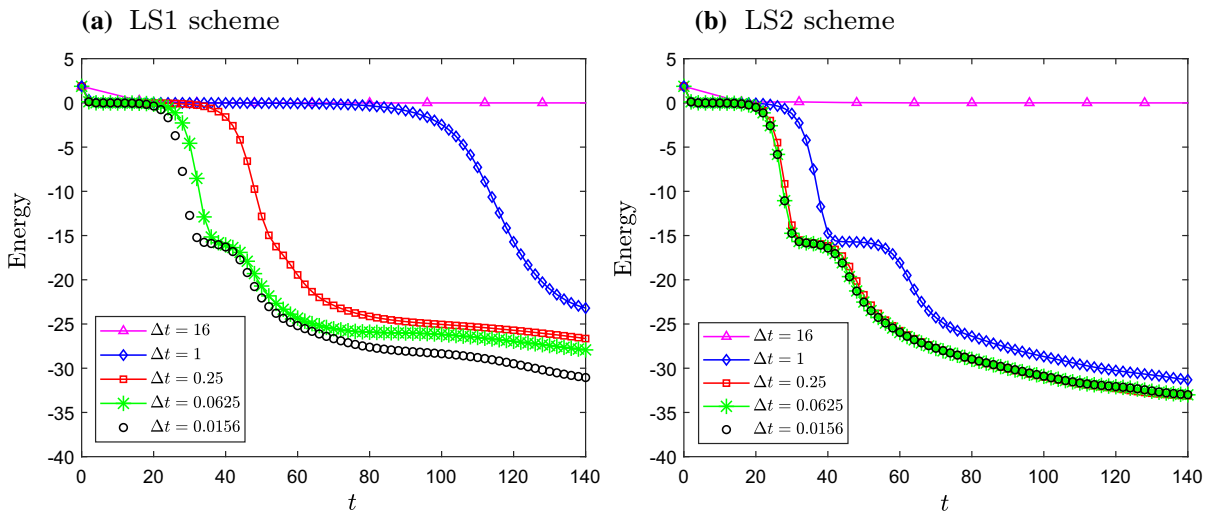


Fig. 1 Temporal evolutions of discrete total energy with respect to **a** LE1 scheme and **b** LS2 scheme

$$\kappa^{n+\frac{1}{2}} = \frac{1}{2}(\Delta\phi^{n+1} + \Delta\phi^n), \tag{20}$$

$$\frac{U^{n+1} - U^n}{\Delta t} = \int_{\Omega} \frac{U^*}{E(\phi^*) + C} F'(\phi^*) \frac{\phi^{n+1} - \phi^n}{\Delta t} d\mathbf{x}, \tag{21}$$

where $\phi^* = \frac{3}{2}\phi^n - \frac{1}{2}\phi^{n-1}$ and $U^* = \frac{3}{2}U^n - \frac{1}{2}U^{n-1}$. Next, we prove the proposed second-order scheme (19)–(21) satisfies the discrete pseudo-energy dissipation law, i.e., $\tilde{\mathcal{E}}(\phi^{n+1}, \phi^n, U^{n+1}) \leq \tilde{\mathcal{E}}(\phi^n, \phi^{n-1}, U^n)$, where

$$\tilde{\mathcal{E}}(\phi^n, \phi^{n-1}, U^n) = U^n + \frac{1}{2}\|\phi^n\|^2 - \|\nabla\phi^n\|^2 + \frac{1}{2}\|\Delta\phi^n\|^2 + \frac{1}{2}\|\nabla(\phi^n - \phi^{n-1})\|^2 - C.$$

By taking the inner product of Eq. (19) with $-(\phi^{n+1} - \phi^n)$, we have

$$-\frac{1}{\Delta t}\|\phi^{n+1} - \phi^n\|^2 = \left(\frac{U^*}{E(\phi^*) + C} F'(\phi^*), \phi^{n+1} - \phi^n\right) + \frac{1}{2}(\|\phi^{n+1}\|^2 - \|\phi^n\|^2) - (\nabla(3\phi^n - \phi^{n-1}), \nabla(\phi^{n+1} - \phi^n)) + (\Delta\kappa^{n+\frac{1}{2}}, \phi^{n+1} - \phi^n), \tag{22}$$

where the integral by parts and periodic boundary condition are used. By using the following identity:

$$(3b - c, a - b) = (a + b - (a - 2b + c), a - b) = |a|^2 - |b|^2 - \frac{1}{2}(|a - b|^2 - |b - c|^2 + |a - 2b + c|^2),$$

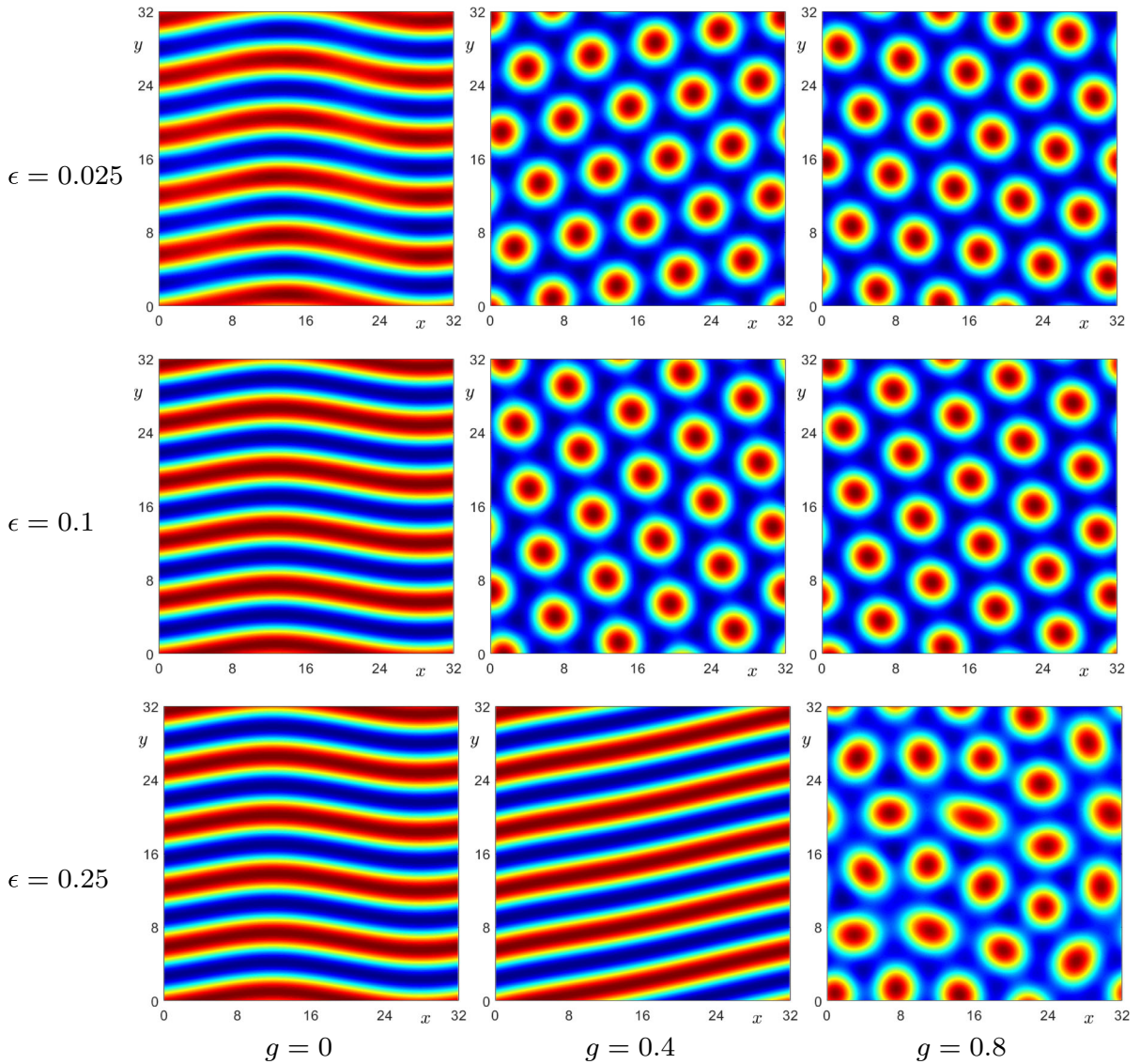


Fig. 2 Effects of numerical parameters on the pattern formations

we can rewrite Eq. (22) to be

$$\begin{aligned}
 -\frac{1}{\Delta t} \|\phi^{n+1} - \phi^n\|^2 &= \left(\frac{U^*}{E(\phi^*) + C} F'(\phi^*), \phi^{n+1} - \phi^n \right) + \frac{1}{2} (\|\phi^{n+1}\|^2 - \|\phi^n\|^2) \\
 &\quad - (\|\nabla \phi^{n+1}\|^2 - \|\nabla \phi^n\|^2 - \frac{1}{2} (\|\nabla(\phi^{n+1} - \phi^n)\|^2 - \|\nabla(\phi^n - \phi^{n-1})\|^2 \\
 &\quad + \|\nabla(\phi^{n+1} - 2\phi^n + \phi^{n-1})\|^2)) + (\Delta \kappa^{n+\frac{1}{2}}, \phi^{n+1} - \phi^n),
 \end{aligned} \tag{23}$$

By using Eq. (20), we have

$$\begin{aligned}
 -\frac{1}{\Delta t} \|\phi^{n+1} - \phi^n\|^2 &= \left(\frac{U^*}{E(\phi^*) + C} F'(\phi^*), \phi^{n+1} - \phi^n \right) + \frac{1}{2} (\|\phi^{n+1}\|^2 - \|\phi^n\|^2) \\
 &\quad - (\|\nabla \phi^{n+1}\|^2 - \|\nabla \phi^n\|^2 - \frac{1}{2} (\|\nabla(\phi^{n+1} - \phi^n)\|^2 - \|\nabla(\phi^n - \phi^{n-1})\|^2)
 \end{aligned}$$

Fig. 3 Temporal evolution of normalized total energy. Here, the final time indicates the numerically steady state

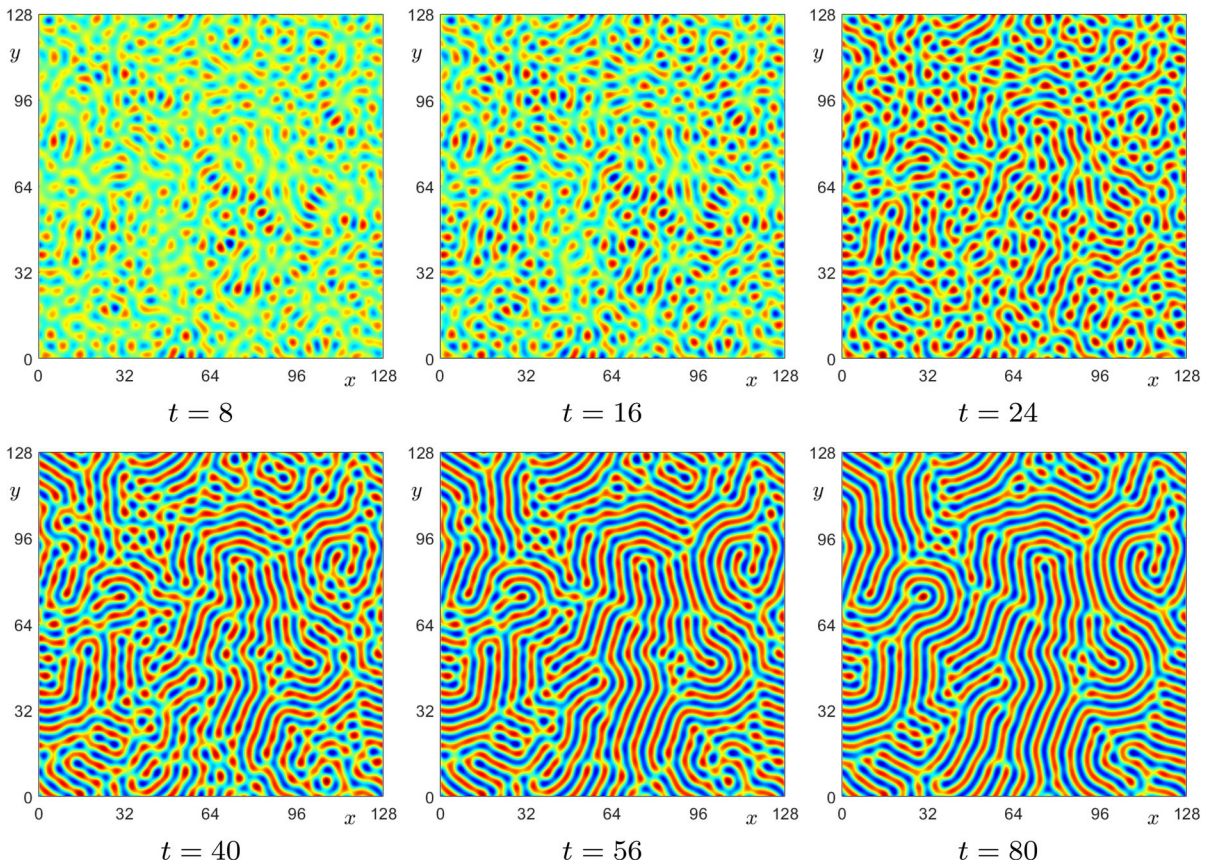
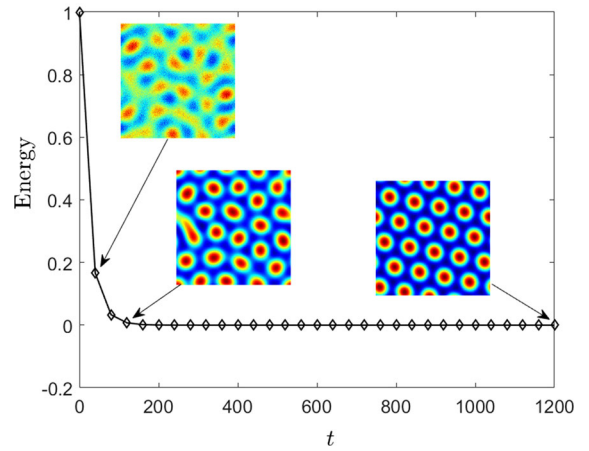


Fig. 4 Temporal evolution of striped pattern

$$+\|\nabla(\phi^{n+1} - 2\phi^n + \phi^{n-1})\|^2) + \frac{1}{2}(\|\nabla\phi^{n+1}\|^2 - \|\nabla\phi^n\|^2), \tag{24}$$

By using Eq. (21), we derive

$$U^{n+1} - U^n + \frac{1}{2}\|\phi^{n+1}\|^2 - \frac{1}{2}\|\phi^n\|^2 - \|\nabla\phi^{n+1}\|^2 + \|\nabla\phi^n\|^2$$

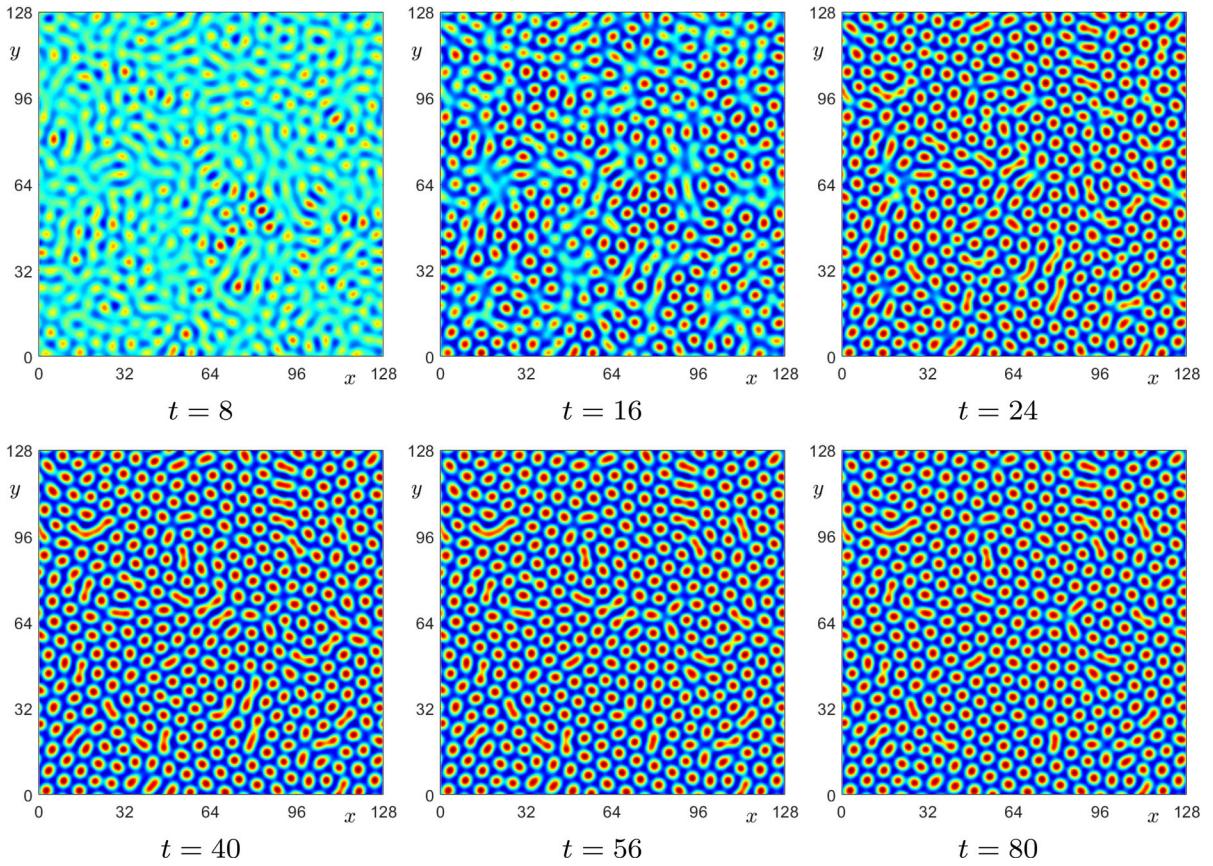
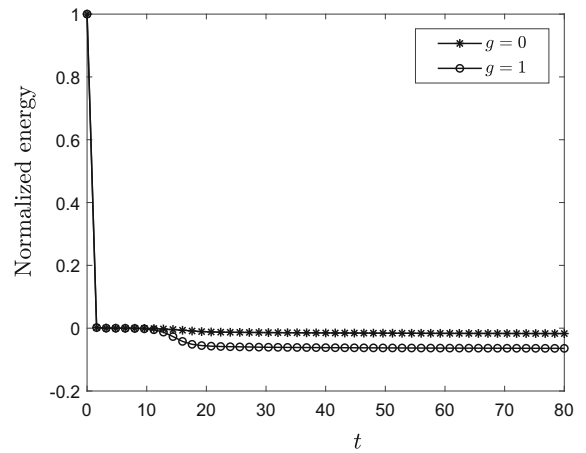


Fig. 5 Temporal evolution of hexagonal pattern

Fig. 6 Temporal evolutions of normalized total energy with respect to different values of g



$$\begin{aligned}
 & + \frac{1}{2} \|\nabla(\phi^{n+1} - \phi^n)\|^2 - \frac{1}{2} \|\nabla(\phi^n - \phi^{n-1})\|^2 + \frac{1}{2} \|\nabla(\phi^{n+1} - 2\phi^n + \phi^{n-1})\|^2 \\
 & + \frac{1}{2} \|\nabla\phi^{n+1}\|^2 - \frac{1}{2} \|\nabla\phi^n\|^2 = -\frac{1}{\Delta t} \|\phi^{n+1} - \phi^n\|^2 \leq 0,
 \end{aligned} \tag{25}$$

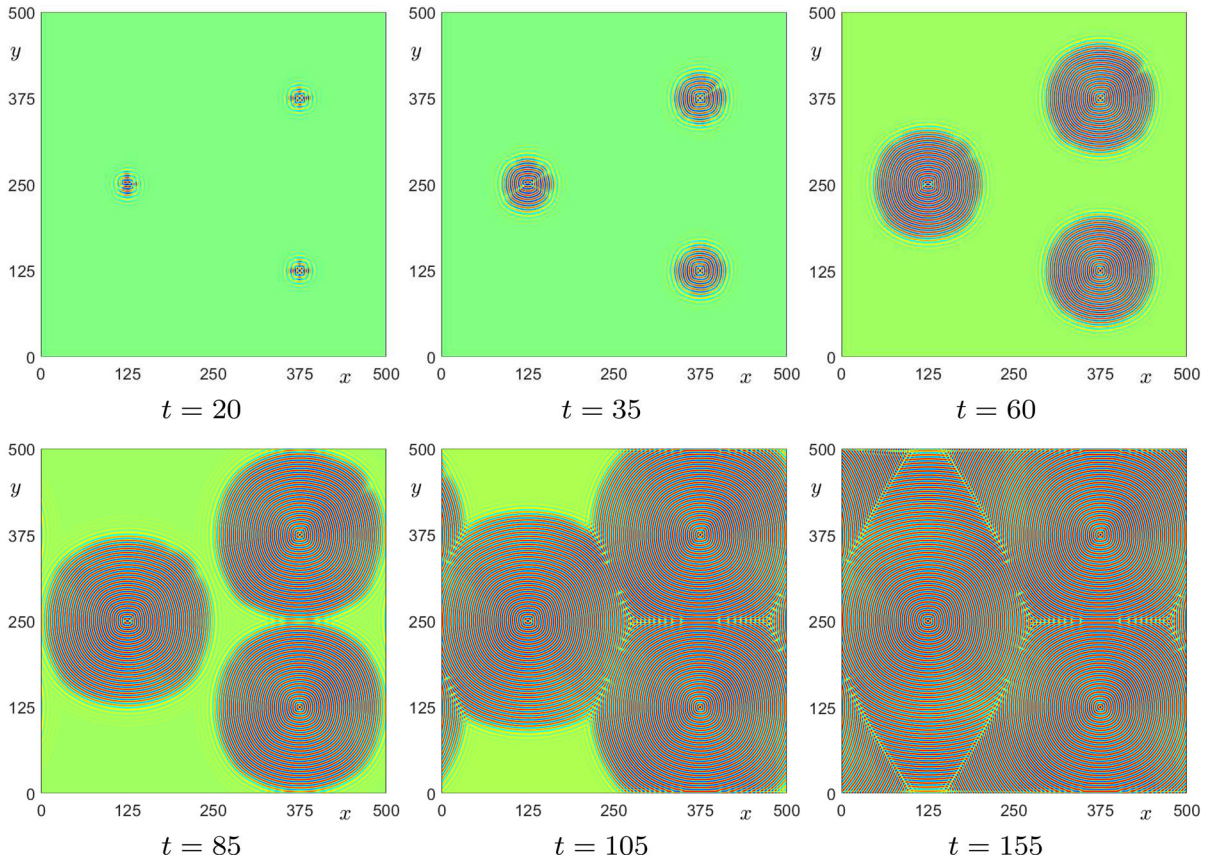


Fig. 7 Temporal evolution of grain growth with $(\epsilon, g) = (0.25, 0)$

which implies $\tilde{\mathcal{E}}(\phi^{n+1}, \phi^n, U^{n+1}) \leq \tilde{\mathcal{E}}(\phi^n, \phi^{n-1}, U^n)$. Moreover, we can easily find that $\tilde{\mathcal{E}}(\phi^n, \phi^{n-1}, U^n) \geq \mathcal{E}(\phi^n, U^n)$. Therefore, we get the following chain of inequalities by assuming $\phi^{-1} \equiv \phi^0$

$$\mathcal{E}(\phi^n, U^n) \leq \tilde{\mathcal{E}}(\phi^n, \phi^{n-1}, U^n) \leq \dots \leq \tilde{\mathcal{E}}(\phi^0, \phi^{-1}, U^0) = \mathcal{E}(\phi^0, U^0), \tag{26}$$

which indicates the total energy at any time level is bounded by the initial energy. The proof is completed.

Remarks We can find that the proposed first- and second-order schemes are both linear systems with constant coefficients. Furthermore, the density field ϕ and auxiliary variable U are decoupled with each other, and thus we can update ϕ by solving only one semi-implicit system and then directly update U by an explicit way. Different with the classical SAV approach, we do not need to calculate the inner product at first; the whole algorithm is significantly simplified. Although our method satisfies the discrete energy dissipation law and does not depend on the positivity restriction which is necessary in the classical SAV method, it is hard for us to theoretically prove the boundedness of discrete energy. The results in Sects. 4.4 and 4.5 show that the total energy is still bounded at the numerical level. In this work, we only focus on the practicability and efficiency of the proposed schemes. To the best of authors' knowledge, the convergence analysis of this modified SAV approach for phase-field models is still an open question. In a recent work of Shen and Xu [38], detailed convergence and error estimations were given for the classical SAV schemes. We will refer to the ideas in [38] to consider the convergence analysis of the proposed schemes for the SH equation and PFC-type equations in the future.

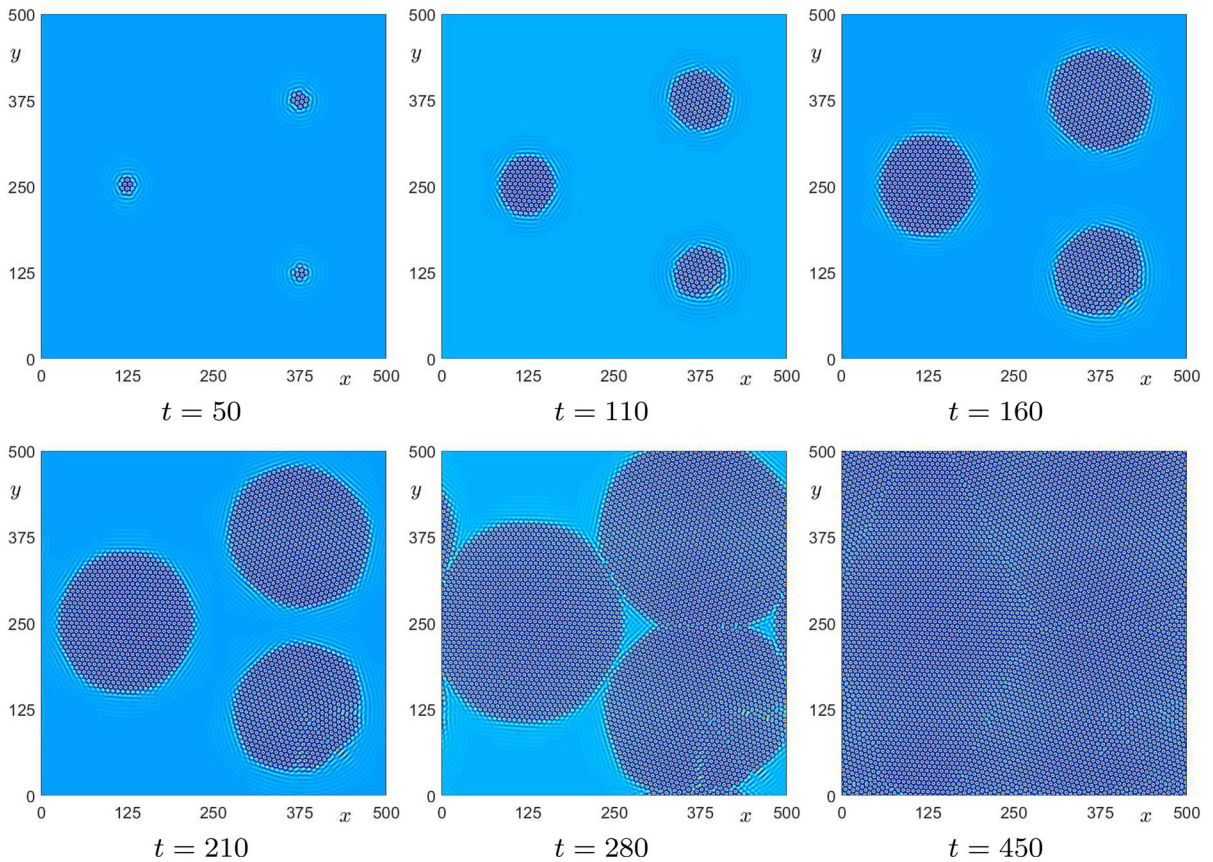


Fig. 8 Temporal evolution of grain growth with $(\epsilon, g) = (0.025, 1)$

4 Numerical experiments

In this work, we only focus on constructing first- and second-order, linear, and energy stable temporal schemes; the standard finite difference method is used to spatially discretize the governing equations and the spatial step is defined as $h = L/N$, where L is the length of computational domain and N is the mesh size. To accelerate the convergence of the resulting linear systems, an efficient linear multigrid algorithm is used. Please refer to [39–41] for some details of multigrid algorithm. In all simulations, we will consider the periodic boundary condition.

4.1 Accuracy test

To verify the desired first- and second-order temporal accuracy of the proposed schemes in Sect. 3, we consider the following initial condition

$$\phi(x, y, 0) = \sin\left(\frac{2\pi}{16}\right) \cos\left(\frac{2\pi}{16}\right) \tag{27}$$

in the domain $\Omega = (0, 32)^2$. The parameters are $h = 0.125$, $\epsilon = 0.25$, $g = 1$. We take the solution with finer time step $\Delta t^r = 0.01h^2$ as the reference solution. The increasing finer time steps: $\Delta t = 320\Delta t^r$, $160\Delta t^r$, $80\Delta t^r$, $40\Delta t^r$, $20\Delta t^r$, and $10\Delta t^r$ are considered. Table 1 illustrates the L^2 -norm errors [42] and convergence rates [42] of ϕ at $t = 0.1$. As we can observe, the desired first- and second-order accuracies can be obtained by using the corresponding LS1 and LS2 schemes.

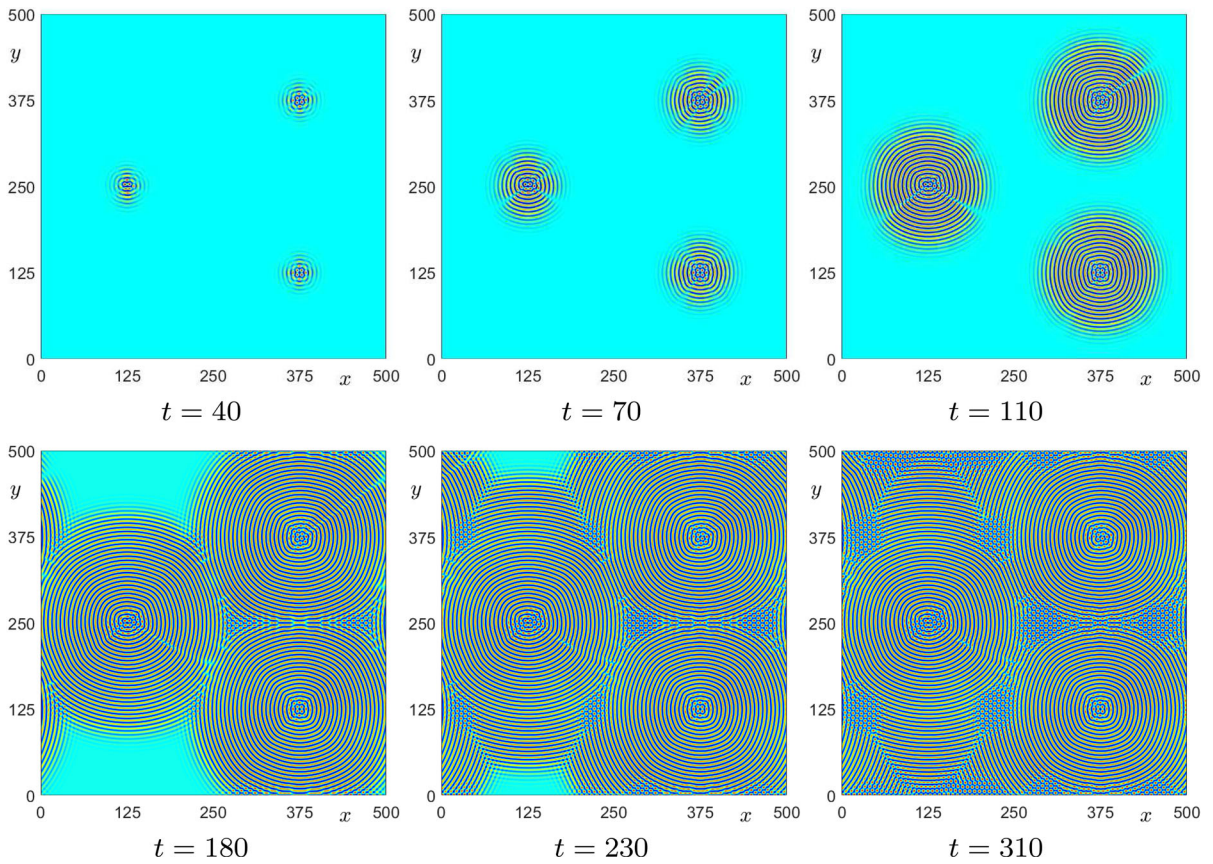


Fig. 9 Temporal evolution of grain growth with $(\epsilon, g) = (0.1, 0.4)$

4.2 Energy stability

To test the energy stability of the proposed LS1 and LS2 schemes, the initial condition [3, 10, 43] is written to be

$$\begin{aligned} \phi(x, y, 0) = & 0.07 - 0.02 \cos\left(\frac{2\pi(x - 12)}{32}\right) \sin\left(\frac{2\pi(y - 1)}{32}\right) \\ & - 0.01 \sin^2\left(\frac{4\pi x}{32}\right) \sin^2\left(\frac{4\pi(y - 6)}{32}\right) \\ & + 0.02 \cos^2\left(\frac{\pi(x + 10)}{32}\right) \sin^2\left(\frac{\pi(y + 3)}{32}\right) \end{aligned} \tag{28}$$

in the domain $\Omega = (0, 32)^2$. We use $h = 0.25$, $\epsilon = 0.25$, and $g = 1$. Figures 1a and b show the temporal evolutions of discrete total energy with respect to the LS1 and LS2 schemes, respectively. We can find that the energy curves are both nonincreasing in time. In the following numerical experiments, the second-order scheme (LS2) will be used for the purpose of better accuracy.

4.3 Effects of numerical parameters

We next consider the effects of numerical parameters (ϵ and g) on the pattern formations in two-dimensional space $\Omega = (0, 32)^2$. We take the initial condition as

$$\phi(x, y, 0) = 0.25 + 0.1 \text{ rand}(x, y), \tag{29}$$

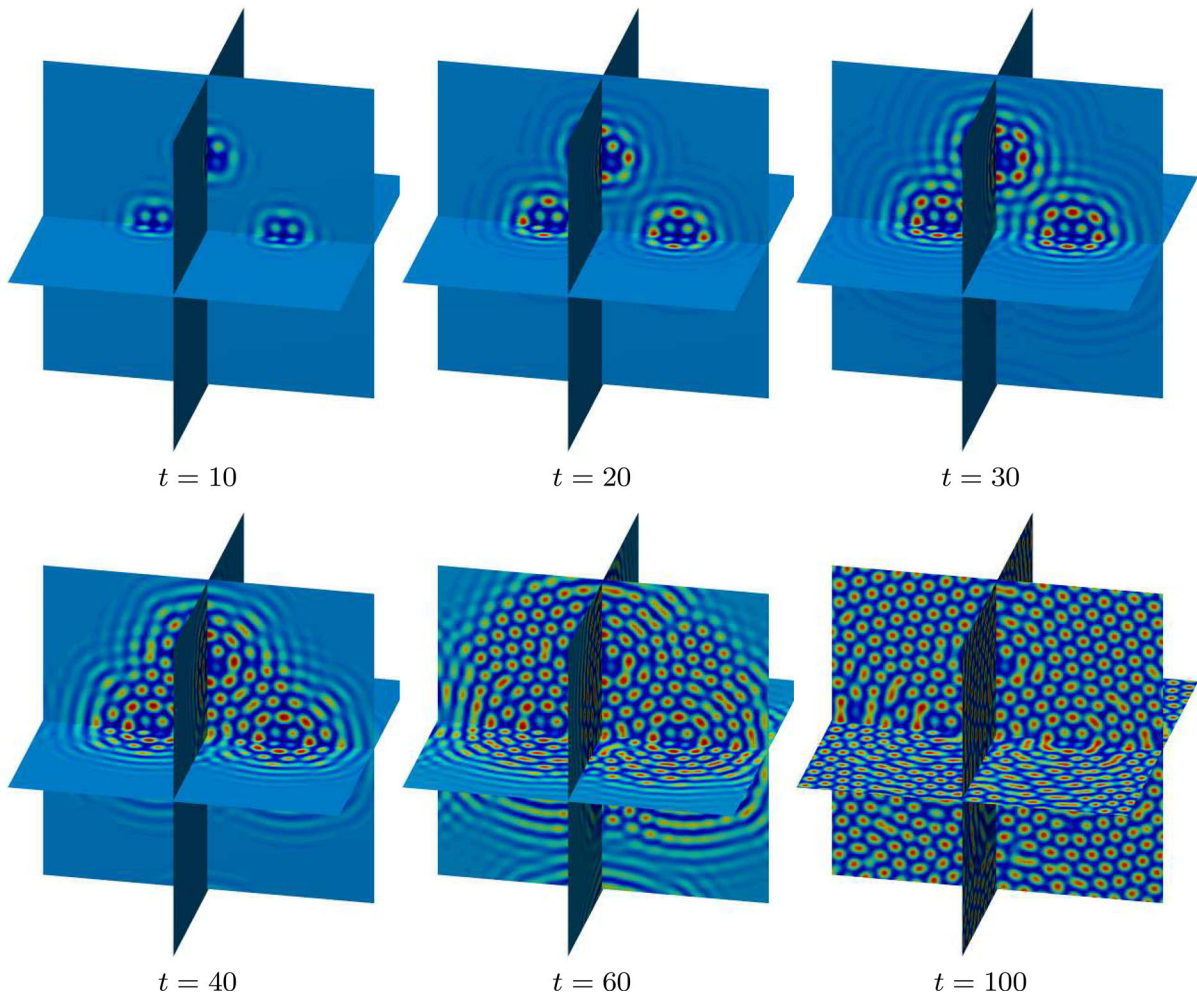


Fig. 10 Temporal evolution of grain growth with $(\epsilon, g) = (0.1, 1)$

where $\text{rand}(x, y)$ is the random number between -1 and 1 . We use $h = 0.125$ and $\Delta t = 1$. Figure 2 presents the profiles with different values of ϵ and g at $t = 512$, and the results indicate that the effect of g is more obvious than the effect of ϵ .

4.4 Long-time simulation of pattern formation

In this subsection, we briefly investigate the energy evolution in a long-time simulation. The computational domain and initial condition are unchanged like those in Sect. 4.3. We use $\epsilon = 0.25$ and $g = 0.8$ to perform the numerical simulation until the steady state, i.e., $\|\phi^{n+1} - \phi^n\|_2 < 10^6$, is arrived. The result in Fig. 3 indicates that the discrete energy functional is nonincreasing and bounded.

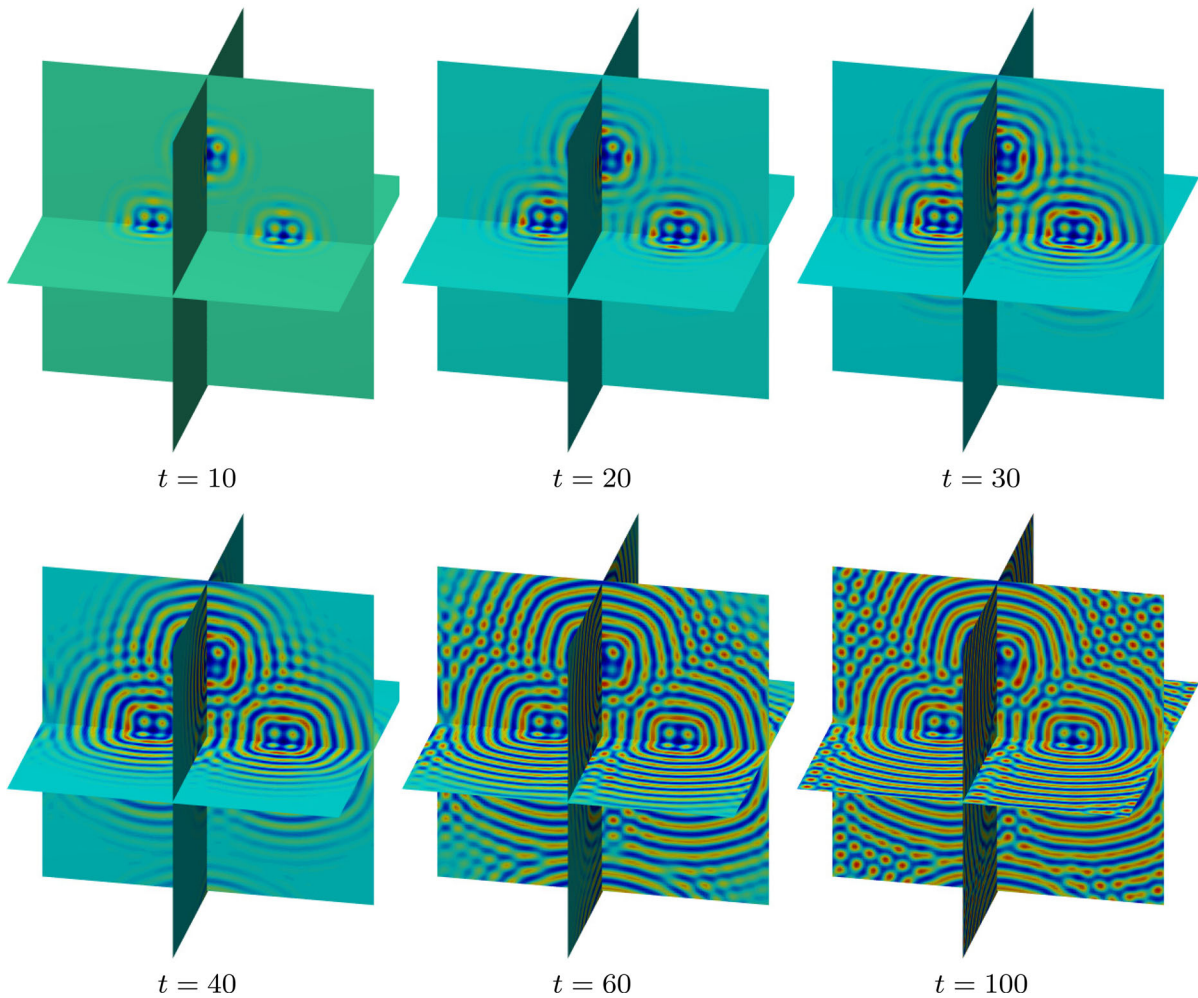


Fig. 11 Temporal evolution of grain growth with $(\epsilon, g) = (0.15, 0.4)$

4.5 Pattern formations in 2D space

In this part, we consider the formations of two typical patterns (striped and hexagonal structures). We take the initial condition to be

$$\phi(x, y, 0) = 0.15 + 0.1 \text{ rand}(x, y), \tag{30}$$

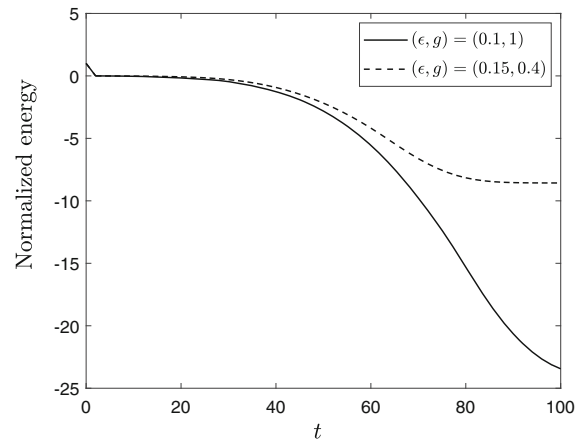
in the domain $\Omega = (0, 128)^2$. We use $h = 0.5$, $\Delta t = 0.1$, and $\epsilon = 0.25$. We consider $g = 0$ and $g = 1$ for the patterns with striped and hexagonal structures, respectively. The temporal evolutions are shown in Figs. 4 and 5. The results in Fig. 6 show that the discrete energy dissipation is satisfied.

4.6 Grain growth in supercooled liquid

Here, we first consider the two-dimensional grain growth in supercooled liquid. The following initial condition is used

$$\phi(x, y, 0) = 0.278 + \alpha \text{ rand}(x, y), \tag{31}$$

Fig. 12 Temporal evolutions of normalized total energy with respect to different values of (ϵ, g)



in the domain $\Omega = (0, 500)^2$. Here, $\alpha = 0.1, 0.2$, and 0.4 for three square nuclei locating at $(375, 125)$, $(375, 375)$, and $(125, 250)$. The length of three square nuclei is 10. The spatial and time steps are set to be $h = 0.9766$ and $\Delta t = 0.1$. The following three sets of parameters $(\epsilon, g) = (0.25, 0)$, $(0.025, 1)$, and $(0.1, 0.4)$ are used to generate different patterns. As shown in Figs. 7, 8, and 9, we can find that the patterns of striped structure, hexagonal structure, and hybrid structure can be generated by manipulating the values of ϵ and g .

Next, we consider the combining effects of ϵ and g on the grain growth in three-dimensional space. The initial condition is taken to be

$$\phi(x, y, z, 0) = 0.278 + \alpha \text{rand}(x, y, z), \quad (32)$$

in the domain $\Omega = (0, 128)^3$. We use $h = 1$ and $\Delta t = 0.1$. Here, $\alpha = 0.1, 0.2$, and 0.4 with respect to three square nuclei locating at $(35, 64, 64)$, $(85, 64, 64)$, and $(64, 64, 95)$, respectively. The length of three nuclei is 10. The following three sets of parameters $(\epsilon, g) = (0.1, 1)$, and $(0.15, 0.4)$ are used. As shown in Figs. 10 and 11, the combining effects of ϵ and g control the formations of hexagonal and striped patterns. The energy curves with respect to different patterns are plotted in Fig. 12, and we find that the energy dissipation law is satisfied.

5 Conclusions

We proposed linear and energy stable numerical schemes for the Swift–Hohenberg equation with $g \geq 0$. A modified SAV approach was used to construct temporally first- and second-order accurate discretizations. Different from the classical SAV approach, the proposed schemes did not need to calculate the inner product at first. We analytically proved the energy stability. The pattern formations in two- and three-dimensional spaces were investigated numerically. The results showed that the proposed scheme gave desired first- and second-order accuracies and energy stability. Note that the proposed schemes can be easily improved by combining a stabilization technique. Because this extension is simple and straightforward, we leave it for interested readers.

Acknowledgements J. Yang is supported by China Scholarship Council (201908260060). The corresponding author (J.S. Kim) was supported by Basic Science Research Program through the National Research Foundation of Korea (NRF) funded by the Ministry of Education (NRF-2019R1A2C1003053). The authors appreciate the reviewers for their constructive comments, which have improved the quality of this paper.

References

1. Swift J, Hohenberg PC (1977) Hydrodynamic fluctuation at the convective instability. *Phys Rev A* 15:319–328
2. Haken H (1983) *Advanced synergetics*. Springer, Berlin

3. Lee HG (2019) An energy stable method for the Swift–Hohenberg equation with quadratic-cubic nonlinearity. *Comput Methods Appl Mech Eng* 343:40–51
4. Hutt A, Atay FM (2005) Analysis nonlocal neural fields for both general and gamma-distributed connectivities. *Physica D* 203:30–54
5. Su J, Fang W, Yu Q, Li Y (2019) Numerical simulation of Swift–Hohenberg equation by the fourth-order compact scheme. *Comput Appl Math* 38:54
6. Kudryashov NA, Sinelshchikov DI (2012) Exact solutions of the Swift–Hohenberg equation with dispersion. *Commun Nonlinear Sci Numer Simul* 17:26–34
7. Xi H, Viñals J, Gunton JD (1991) Numerical solution of the Swift–Hohenberg equation in two dimensions. *Physica A* 177:356–365
8. Christov CI, Pontes J (2002) Numerical scheme for Swift–Hohenberg equation with strict implementation of Lyapunov functional. *Math Comput Model* 35:87–99
9. Gomez H, Nogueira X (2012) A new space-time discretization for the Swift–Hohenberg equation that strictly respects the Lyapunov functional. *Commun Nonlinear Sci Numer Simul* 17:4930–4946
10. Nikolay NA, Ryabov PN (2016) Analytical and numerical solutions of the generalized dispersive Swift–Hohenberg equation. *Appl Math Comput* 286:171–177
11. Dehghan M, Abbaszadeh M (2017) The meshless local collocation method for solving multi-dimensional Cahn–Hilliard, Swift–Hohenberg and phase field crystal equations. *Eng Anal Bound Elem* 78:49–64
12. Abbaszadeh M, Khodadadian A, Parvizi M, Dehghan M, Heitzinger C (2019) A direct meshless local collocation method for solving stochastic Cahn–Hilliard–Cook and stochastic Swift–Hohenberg equations. *Eng Anal Bound Elem* 98:253–264
13. Sarmiento AF, Espath LFR, Vignal P, Dalcin L, Parsani M, Calo VM (2018) An energy-stable generalized- α method for the Swift–Hohenberg equation. *J Comput Appl Math* 344:836–851
14. Lee HG (2017) A semi-analytical Fourier spectral method for the Swift–Hohenberg equation. *Comput Math Appl* 74:1885–1896
15. Wise SM, Wang C, Lowengrub JS (2009) An energy-stable and convergent finite-difference scheme for the phase field crystal equation. *SIAM J Numer Anal* 47(3):2269–2288
16. Hu Z, Wise SM, Wang C, Lowengrub JS (2009) Stable and efficient finite-difference nonlinear-multigrid schemes for the phase field crystal equation. *J Comput Phys* 228:5323–5339
17. Guan Z, Heinonen V, Lowengrub J, Wang C, Wise SM (2016) An energy stable, hexagonal finite difference scheme for the 2D phase field crystal amplitude equations. *J Comput Phys* 321(15):1026–1054
18. Wang C, Wise SM (2011) An energy stable and convergent finite-difference scheme for the modified phase field crystal equation. *SIAM J Numer Anal* 49(3):945–969
19. Baskaran A, Hu Z, Lowengrub JS, Wang C, Wise SM, Zhou P (2013) Energy stable and efficient finite-difference nonlinear multigrid schemes for the modified phase field crystal equation. *J Comput Phys* 250(1):270–292
20. Cheng K, Wang C, Wise SM (2019) An energy stable BDF2 Fourier pseudo-spectral numerical scheme for the square phase field crystal equation. *Commun Comput Phys* 26(5):1335–1364
21. Baskaran A, Lowengrub JS, Wang C, Wise SM (2013) Convergence analysis of a second order convex splitting scheme for the modified phase field crystal equation. *SIAM J Numer Anal* 51(5):2851–2873
22. Dong L, Feng W, Wang C, Wise SM, Zhang Z (2018) Convergence analysis and numerical implementation of a second order numerical scheme for the three-dimensional phase field crystal equation. *Comput Math Appl* 75(6):1912–1928
23. Long J, Luo C, Yu Q, Li Y (2019) An unconditionally stable compact fourth-order finite difference scheme for three dimensional Allen–Cahn equation. *Comput Math Appl* 77(4):1042–1054
24. Hou T, Tang T, Yang J (2017) Numerical analysis of fully discretized Crank–Nicolson scheme for fractional-in-space Allen–Cahn equations. *J Sci Comput* 72:1214–1231
25. Liao HL, Tang T, Zhou T (2020) A second-order and nonuniform time-stepping maximum-principle preserving scheme for time-fractional Allen–Cahn equations. *J Comput Phys* 414(1):109473
26. Grillo A, Carfagna M, Federico S (2018) An Allen–Cahn approach to the remodelling of fibre-reinforced anisotropic materials. *J Eng Math* 109:139–172
27. Cheng K, Feng W, Wang C, Wise SM (2019) An energy stable fourth order finite difference scheme for the Cahn–Hilliard equation. *J Comput Appl Math* 362(15):574–595
28. Yang J, Li Y, Lee C, Jeong D, Kim J (2019) A conservative finite difference scheme for the N -component Cahn–Hilliard system on curved surfaces in 3D. *J Eng Math* 119:149–166
29. Li Q, Mei L, You B (2018) A second-order, unquely solvable, energy stable BDF numerical scheme for the phase field crystal model. *Appl Numer Math* 134:46–65
30. Guillén-González F, Tierra G (2013) On linear schemes for the Cahn–Hilliard diffuse interface model. *J Comput Phys* 234:140–171
31. Liu Z, Li X (2019) Efficient modified stabilized invariant energy quadratization approaches for phase-field crystal equation. *Numer Algorithms* 85:107–132
32. Li Q, Mei L (2020) Efficient, decoupled, and second-order unconditionally energy stable numerical schemes for the coupled Cahn–Hilliard system in copolymer/homopolymer mixtures. *Comput Phys Commun* 260:107290
33. Yang X, Han D (2017) Linearly first- and second-order, unconditionally energy stable schemes for the phase field crystal model. *J Comput Phys* 330(1):1116–1134
34. Liu Z (2019) Efficient invariant energy quadratization and scalar auxiliary variable approaches without bounded below restriction for phase field models. *arXiv preprint*

35. Liu Z, Li X (2019) Step-by-step solving schemes based on scalar auxiliary variable and invariant energy quadratization approaches for gradient flows. arXiv preprint
36. Yang J, Kim J (2020) An improved scalar auxiliary variable (SAV) approach for the phase-field surfactant model. *Appl Math Model* 90:11–29
37. Espath L, Calo VM, Fried E (2020) Generalized Swift–Hohenberg and phase-field-crystal equations based on a second-gradient phase-field theory. *Meccanica* 55:1853–1868
38. Shen J, Xu J (2018) Convergence and error analysis for the scalar auxiliary variable (SAV) schemes to gradient flows. *SIAM J Numer Anal* 56:2895–2912
39. Kim J, Kang K, Lowengrub J (2004) Conservative multigrid methods for the Cahn–Hilliard fluids. *J Comput Phys* 193:511–543
40. Wise S, Kim J, Lowengrub J (2007) Solving the regularized, strongly anisotropic Cahn–Hilliard equation by an adaptive nonlinear multigrid method. *J Comput Phys* 226:414–446
41. Feng W, Guo Z, Lowengrub JS, Wise SM (2018) A mass-conservative adaptive FAS multigrid solver for cell-centered finite difference methods on block-structured locally-cartesian grids. *J Comput Phys* 352:463–497
42. Yang J, Kim J (2020) An unconditionally stable second-order accurate method for systems of Cahn–Hilliard equations. *Commun Nonlinear Sci Numer Simul* 87:105276
43. Baskaran A, Hu Z, Lowengrub JS, Wang C, Wise SM, Zhou P (2013) Energy stable and efficient finite-difference nonlinear multigrid schemes for the modified phase field crystal equation. *J Comput Phys* 250:270–292

Publisher's Note Springer Nature remains neutral with regard to jurisdictional claims in published maps and institutional affiliations.